Thin Cambered Lifting Bodies in Ground Effect Flight

Galen J. Suppes[1] and Adam B. Suppes[2]
HS-Drone LLC, Charlottesville, VA 22911

Ground effect flight uses the ground to block downward dispersion of lift pressures, increasing both lift and lift-drag-ratios (L/D). For thin-cambered wing sections, L/D increases as the ratio of the wing sections frontal projected height to ground clearance with the ground increases. This allows thin cambered panels at higher cambers (e.g. 6%) to operate at high L/D with reasonable clearances of water and ground. Functionally, a thin cambered mid-section of a wing-in-ground (WIG) aircraft delivers more lift per mass than a wing and can replace laterally-extending wings in WIG platforms with frames that allow the tensile strength of the panel to transfer lift forces to the rest of the aircraft. A catamaran airship design emerges where, with minimal weight penalties, an inboard thin cambered wing is able to: a) increase lift, b) increase surface area for solar power collection, and c) provide a low-resistance path for crossover propulsor benefits in transition from hovering to aerodynamic lifting-body flight. This paper evaluates the performance of thin-cambered inboard sections for ground-effect machines.

Nomenclature

2D = two dimensional.
3D = three Dimensional.
AR = aspect ratio, defined as the span divided by a representative longitudinal chord length.
Camber = curvature of an wing section characterized as a deviation from straight as either a fraction of the chord length or percent of a chord length (e.g., 0.01 c or 1%).
CFD = computational fluid dynamics.
c, Chord = chord, distance from leading edge to trailing edge of an wing section or wing.
Clearance = The distance of closest approach of an wing section component to stationary object.
Clearance Ratio = Ratio of the distance between the lowest part of the fence and the ground divided by the wing section thickness; the wing section thickness does not include the fence or flap.
$Drag_{form}$ = form drag, which herein is the drag due to pressure on the surface.
$Drag_{total}$ = total drag as equal to sum of form and shear drag
Gap Ratio = Ratio of wing section thickness to the distance between the lowest part of the wing section and the ground; for this definition the flap and fence are not considered part of the wing section.

[1] Chief Engineer, Homeland Technologies, LLC, gjsuppes@gmail.com
[2] Senior Research Engineer, Homeland Technologies, LLC

L/D = lift-drag ratio, the primary measure of airframe efficiency; ***L/D*** is calculated as the CFD lift coefficient divided by the drag coefficient.

lift pressures = pressures that generate aerodynamic lift such as lower pressures on upper surfaces and higher pressures on lower surfaces.

NACA0006 = an wing section shape defined by NACA standards with a t/c of 0.06

P = pressure (N/m^2)

% Flap = Flap extension as fraction of fence: where 0% is trailing edge of the flap even with the lowest part of the wing section, 100% is trailing edge of the flap is even with the lowest part of the fence.

S, dS = surface area (m^2) and differential surface area

STL = stereolithography, file generated by computer aided design software

U, ***u*** = velocity.

t/c = thickness to chord ratio, thickness is a maximum vertical dimension

VTOL = vertical takeoff and landing.

α_A = angle from horizontal (°), subscript A identifies an wing section pitch angle with nose up as positive.

α_P = angle from horizontal (°), subscript P identifies angle of a point on a line or surface.

Introduction

For nearly a century, ground-effect aircraft have been stuck in a paradigm of incrementally improved efficiency (e.g., 25% increase) over free-flight counterparts [1, 2]. Recent work has a revised approach to design with computational fluid dynamics (CFD) identifying multiple applications able to achieve L/D efficiencies >200% the efficiencies of free-flight counterparts in low-aspect-ratio ground effect machines (GEM) [3]. For present purposes, GEM are platforms capable of both hovercraft and wing in ground (WIG) flight.

Marginally-useful simple explanations of how air flow creates aerodynamic lift in contemporary fixed-wing aircraft are ineffective in either explanation or extrapolation of GEM designs. However, an airfoil science based on the following three basic principles of physics has enabled multiple innovations on this subject:

Principle 1. Impacting air flows create higher surface pressures.

Principle 2. Diverging air flows create lower surface pressures.

Principle 3. Air flowing from higher to lower pressures at the speed of sound extends lift pressures along streamlines, dissipates lift pressures across streamlines, and interacts with air flow to turn streamlines.

Three additional principles guide in the design of lifting bodies to place the lift pressures on the wing section to create high L/D efficiency:

Principle 4. The L/D of a section of an airplane surface is approximately equal to 57° divided by the pitch of the surface in degrees for lower surfaces and -57° divided by the pitch for upper surfaces. The pitch angle is relative to horizontal with the nose up as positive.

Principle 5. Surfaces can be used to block loss of lift pressures leading to increased L/D. Example surfaces are winglets on wings and fences under lifting bodies.

Principle 6. For a ground-effect aircraft with a properly-designed lower fenced cavity, 3D CFD estimates of cavity lift pressures are able to approach 2D estimates, enabling 2D wing section simulations to accurately predict actual performances in many applications.

These principles challenge schools of thought on ground effect flight which focused on: i) deriving analytical expressions, ii) reducing induced drag, iii) correlating increasing flight efficiency with increasing chord length, iv) analyzing velocity profiles, and v) using wings to generate aerodynamic lift [4]. Figure 1 illustrates the base case ground-effect flight transit (GEFT) vehicle of instant research which is a GEM design. GEFT technology is a result of technology which focuses on: i) extrapolating CFD simulation results, ii) increasing aerodynamic lift, iii) correlating flight efficiency with increasing lifting body thickness, iv) analyzing pressure profiles, and v) using the lower surfaces of lifting bodies to generate aerodynamic lift.

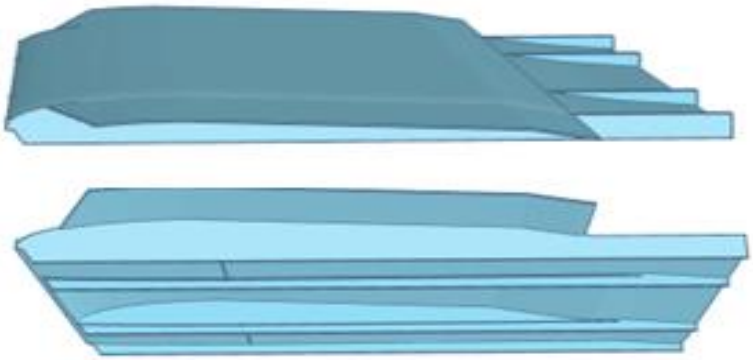

Figure 1. Digital prototype of HS-Drone ground-effect aircraft using a thin cambered-panel inboard section and flat-bottom outboard sections. A lower cavity is defined by two pairs of fences and a trailing flap where the cavity below the thin cambered panel is part of the cavity.

In water, the Figure 1 GEFT has a catamaran-type hull/fuselage configuration with a thin cambered inboard platform. Single-sheet thin-camber designs are possible in designs like kites, paragliders, and hang-gliders where tensile forces of the sheet transfer lift forces to leading and trailing crossbars. The thin cambered section provides a light-weight and possibly spanwise expandable section which can change the vehicle shape from one more-robust against tidal forces to one with greater lift. This paper reports CFD simulations of thin cambered wing sections and digital prototype performances of GEFT of the Figure 1 design.

Background

Traditional schools of thought on WIG aircraft have emphasized flight over water where the water reduces induced drag on the aircraft. This is attributed primarily to the ground or water obstructing the creation of wingtip vortices and interrupting downwash behind the wing [5, 6]. Implicit in this analysis is the use of wings rather than lifting bodies. Figure 2 compares the GEFT planform to three planforms resulting from decades of planform evolution based on this approach.

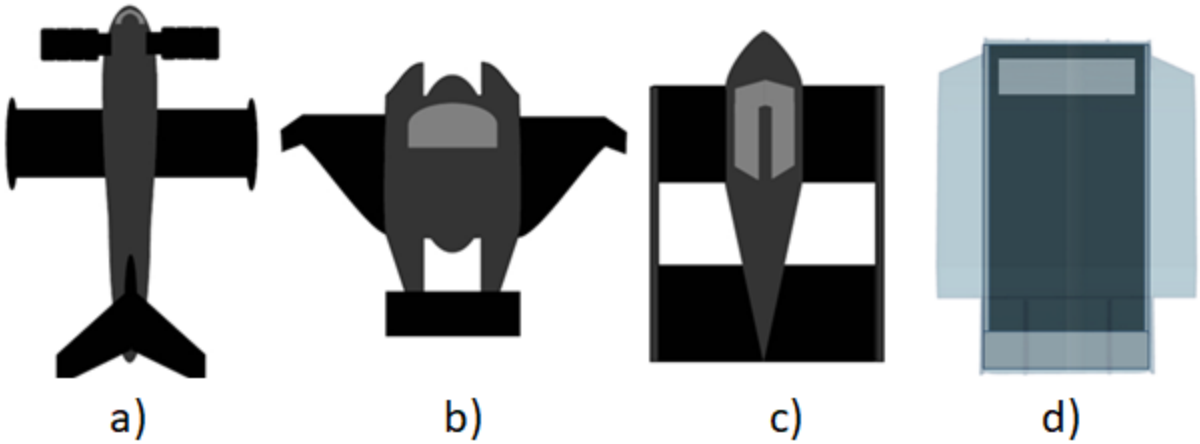

Figure 2. Planforms of WIG designs: a) USSR ekranoplan (1980's), b) Airfish 8 (2024), and c) Regent (2024) and lifting body design d) Ground Effect Machine (GEM) [7-10].

In the early work (i.e., December-2023), simulations were performed on a flying vehicle with the objective of using the rails to block spanwise loss of lift pressures. These exploratory studies were a result of past interest tethered-flight guideway transit and approaches to increase lift generation on low-aspect-ratio aerial-towed-platform aircraft [11, 12].The authors learned that the blocking of downward dissipation of lift forces has as much an impact on L/D efficiency as blocking lateral loss of lift pressures.

Terms like "downwash", "induced drag", and "wing vortex" can be applied differentially, while the term "dissipation" of lift pressures covers the all the loss phenomena. Dissipation tends to be in all directions that are not blocked by surfaces, and surfaces implicitly block the dissipation. The insight was gained from observing trends in CFD simulations [3, 13]. The source of pressure's extension of beneficial lift pressures and the dissipation/loss of lift pressures becomes is explicit in the Navier-Stokes equation (Equations 1 and 2) taken at the limit of zero viscosity, two dimensions, and at a mesh location removed from a wing section surface.

$$\rho\left(\frac{\partial u}{\partial t} + u\nabla \mathrm{u}\right) = -\nabla \mathrm{p} \tag{1}$$

Where:

$$\nabla \mathrm{u} = \begin{bmatrix} \frac{\partial u}{\partial x} \\ \frac{\partial u}{\partial y} \end{bmatrix} \tag{2}$$

$$\nabla \mathrm{p} = \begin{bmatrix} \frac{\partial p}{\partial x} \\ \frac{\partial p}{\partial y} \end{bmatrix} \tag{3}$$

Within a streamline of air flow, pressure gradients can lead to changes in velocity gradients and vice-versa—an energy conversion often associated with the Bernoulli equation. Across streamlines, pressure gradients lead to the upward or downward flow of velocity which is lost work when that velocity results in mixing—at the microscopic diffusion level or macroscopic turbulent level.

The Figure 1 base case design is a lifting body design that emphasizes lift forces on the lower surface and incorporates the following features [8]:

1. A lower surface is relatively flat to maximize L/D per Principle 4.
2. A trailing flap generates higher pressures (Principle 1) which extend forward along the lower surface when dissipation is blocked (Principle 3).
3. Fences along the sides of a lower cavity block spanwise dissipation (Principle 5).
4. The leading section is designed to provide induced thrust.
5. Lift-Span Tech is used to enhance induced thrust and alleviate induced drag.
6. A lifting body design is used to maximize lift as described by the following paragraphs.
7. A thin cambered inboard platform between two side fuselages resembling a catamaran's twin hulls with inboard trampoline and crossbars.

Other studies have reported the approach to GEFT design and example wing section pressure profiles such as summarized by Figures 3 and 4 [14, 15]. Figure 3 identifies how lift forces on the lower surface increase as the wing section approaches the ground. Figure 4 identifies how the lift forces are greater for a thicker wing section than a very thin wing section.

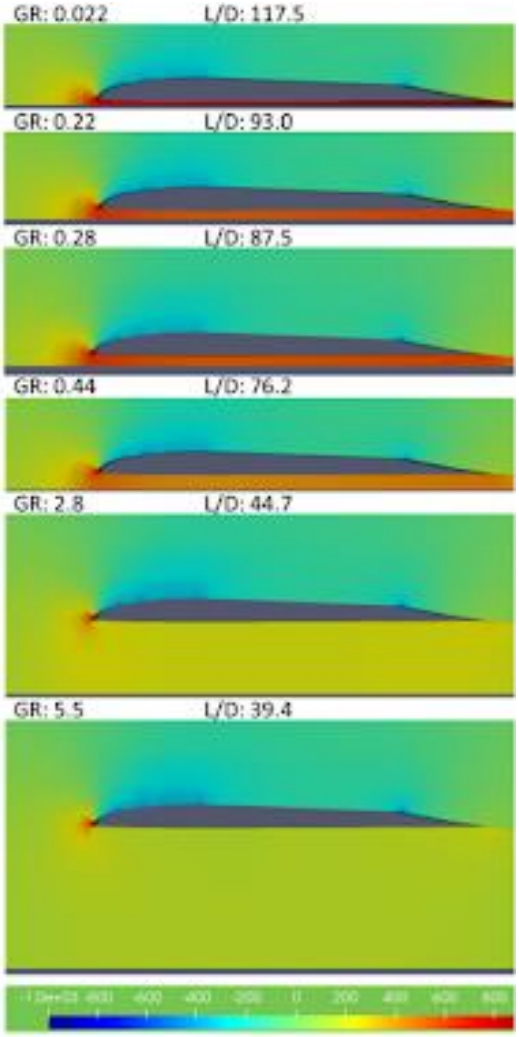

Figure 3. Pressure profiles of early wing sections as a function of gap ratio (i.e., ratio of gap with ground to wing section thickness).

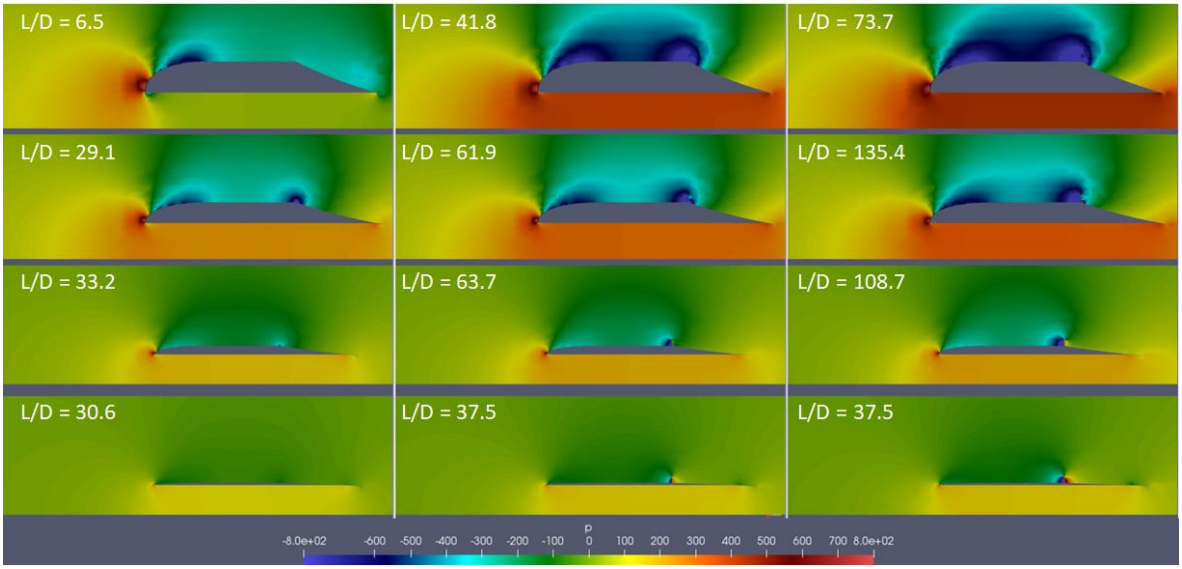

Figure 4. Pressure profiles for a wing section at Source settings of 0, 2.5, and 5 m^4/s^2.

Also, Figure 4 identifies how prominent leading and trailing stagnation points correlate with high L/D efficiency; when both are present, the forward and rearward expansion of pressure forces leads to a constant and prominent lower surface lift pressure. The greater the expanse of the forward stagnation point, the greater the availability of extension of the higher pressure along the lower surface.

Figure 4 conveys a correlation between wing section thickness with both lift and L/D efficiency. Traditional schools of thought identify a correlation of L/D efficiency with wing section chord length. The current correlation with wing section thickness, or thickness-to-chord ratio, manifests when distributed propulsion interacts with the wing section surface to both enhance induced thrust and nullify induced drag. It is not a single issue; but rather coupled issues. In the complexity of coupled issues, fundamentally correct principles can guide design while empirical correlations are rarely accurate.

Work of Bulat et al. – The work of Bulat et al stands out as having similar timelines as the current research and development, a superficially-similar wing section (Figure 5), and application of distributed propulsion (Figure 5) toward advancing ground-effect flight [4]. Their studies emphasized alleviating boundary-layer separation on the M06 wing section and comparing the accuracy of different CFD turbulence models.

Figure 5. Aerodynamic Wing section E387, M06-13-128 [4].

The current work arrived at the use of Lift-Span Tech distributed propulsion as a result of basic studies on the best location of distributed propulsion with adjustment to accommodate thicker wing sections [16]. Distributed propulsion is simulated as source of velocity which inherently generates lower pressures at the propulsor intake and higher pressures at the discharge. A benefit of this approach is the propulsor separating the aerodynamics of the “Lift Span” surface forward of the propulsor from the tapered upper surface aft of the propulsor. For the thickest wing section of Figure 4 at a zero Source setting, the L/D with boundary layer separation is 6.5. Even a low setting (i.e. 2.5 m^4/s^2) suppresses or reduces boundary layer separation with a marked increase in L/D to 41.8.

The form drag of a thick wing section with a steep trailing taper can be significant. The design criteria of GEFT technology is to operate the trailing taper’s pitch in combination with the Lift-Span propulsor to generate near-free-stream pressure to avoid generation of form drag. The optimal surface shape of both the Lift Span and the trailing paper will vary with propulsor power output; and so, both are preferably morphing surfaces that respond to propulsor power.

This paper extends upon previous work on GEFT with an emphasis on comparing different turbulence models, similar to the rigor of Bulat et al. The paper extends GEFT studies to include a cross-over propulsors and the use of inboard platforms.

Thin Cambered Wing sections – Thin cambered wing sections can have particular utility as light-weight inboard platforms for ground effect aircraft and solar aircraft when combined with bifacial panel technology [17-19]. Figure 6 compares the pressure profiles of a 0.01 camber to a 0.06 camber wing section.

The comparison illustrates how an increase in camber of thin cambered wing sections can lead to considerable increases in lift while maintaining reasonable L/D efficiency. The primary reason the 0.06 camber wing section is able to maintain high L/D efficiency—in view of Principle 4—is that surface pressures for the forward half of the wing section generate forward forces (i.e., thrust). Those forward forces substantially cancel the form drag from the aftward portion of the wing section. Principles 1-3 explain how the lift forces are generated and how they expand throughout the wing section.

Structural weakness and lateral dissipation of lift forces limit practical applications of thin cambered wing sections. However, within a frame, tensile strength is enough to support thin cambered wing sections and to transfer the lift to aircraft crossbars; this is the approach used with hang gliders and the digital prototype of Figure 1. Lower surface fences or outboard fuselage sections are able to reduce losses of lower surface lift pressures.

A synergy emerges with GEFT aircraft where fences enable both higher L/D and the use of mid-section thin cambered panels to increase lift with low weight penalties.

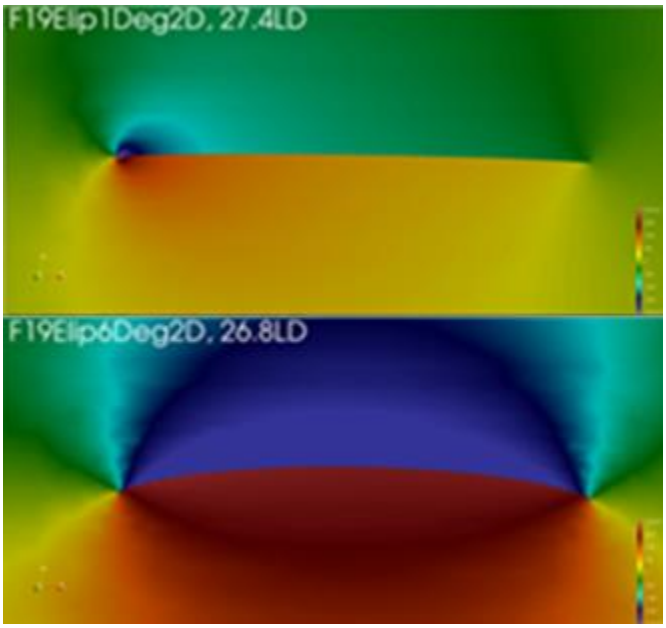

Figure 6. Comparison of 0.01 to 0.06 elliptic camber wing sections.

Distributed Propulsion– Propellers and fans (i.e., Sources) create lower pressures on forward surfaces and higher pressures on rearward surfaces. And since surfaces are required to support propellers and fans, good design teaches toward placement of Sources to generate lift from their local aerodynamics—so long as there is minimal interference with engine thrust [16, 20-26]. Figure 7 illustrates the impact of how a Source can modify the pressure profile on a flat plate. Table 1 provides the lift coefficients and L/D efficiency.

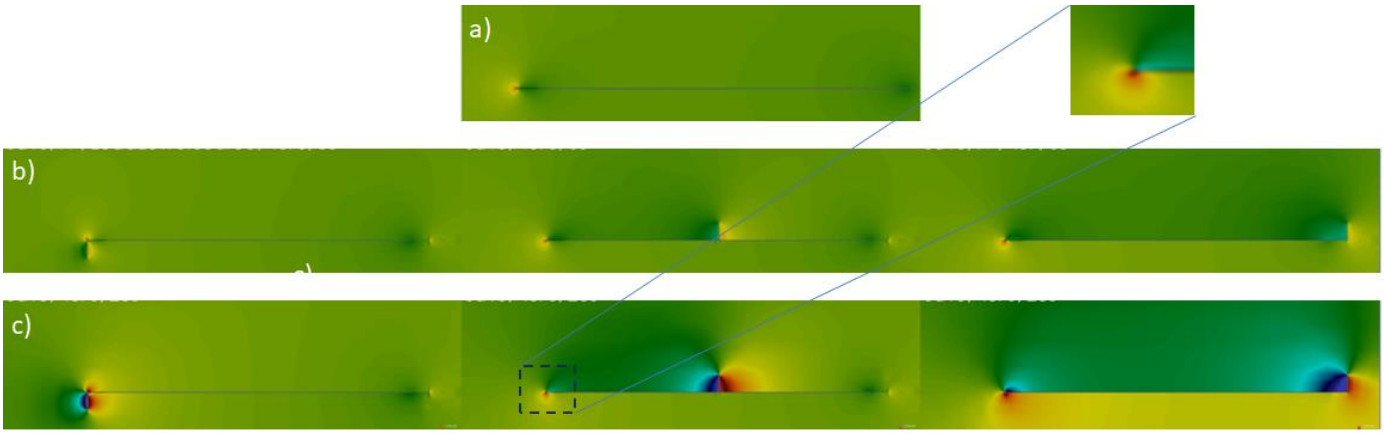

Figure 7. Pressure profiles of propulsion sources on thin flat plate wing section at propulsor settings of: a) 0, b) 5, and c) 20. From left to right propulsors are leading edge, mid-section, and trailing edge. See Figure 5 for pressure scale.

Table 1. Performance of propulsion sources on flat plate wing section.

Prop		Prop.	Upper Propulsor			Lower Propulsor		
Lead /Trail	**Pitch**	**Power**	**Cl**	**Cd**	**L/D**	**Cl**	**Cd**	**L/D**
0	0	0	0.00	0.00	0			
Lead	0	20	-0.0054	0.0112	-0.5	0.0054	0.0112	0.5
Mid	0	20	0.0076	0.0089	0.8	-0.0076	0.0089	-0.8
Trail	0	20	0.1740	0.0080	**21.8**	-0.1740	0.0080	-21.8
0	1	0	0.0891	0.0090	9.9			
Trail	1	20	0.2840	0.0121	**23.5**	0.0894	0.0133	6.7
0	3	0	0.2830	0.0215	13.2			
Trail	3	20	0.4910	0.0324	**15.2**	0.2960	0.0261	11.3
Middle Propulsor								
Afore	3	80	0.3080	0.0290	10.6			
Afore	3	200	0.3370	0.0413	8.2			

The flat plate provides a good surrogate for fundamental insight due to the absence of curved surfaces complicating interpretations and presence of vertical symmetry allowing more concise summaries of impact. For example, the L/D of a trailing-edge propulsor on the upper surface is 21.8 while on the lower surface it is -21.8. The

propulsion sources were most effective for increasing L/D when on the upper surface of the trailing edge with modest benefit on the upper surface midsection.

When a propulsion source is placed afore a leading edge of a wing section at a modest pitch, the discharge can impact the lower surface and create a moderate increase in L/D. This forward "tractor" position is common with WIG aircraft since it can decrease the speed at which full aerodynamic lift is attained; however, the fundamental data of Table 1 identifies that the upper surface pusher position provides both higher lift coefficients and higher L/D.

A pitfall of tractor propulsion is that the higher pitch angles needed to increase the lift coefficient come at the cost of higher form drag (i.e., Principle 4). This limits the upside potential of tractor propulsion with WIG aircraft. Otherwise, it is reasonable to pursue L/D in excess of 30.

Wing sections with convex-upward upper surfaces are prevalent, and upper surface pitches in excess of 2° at the trailing edge are common. Preliminary studies have identified that the best overall performance is achieved with trailing edge surfaces that morph to reduce surface pitches as the power of a pusher propulsor increases [17, 16, 27, 13, 3]. There are also opportunities for upper surface midsection propulsion sources to create lower pressures on zero to negative degree pitch upper surfaces with extended benefits. These topics are part of the Discussion of this paper.

Methods

2D CFD calculations were performed using SimFlow's Wing section simulation feature. 3D CFD calculations were performed in OpenFoam. The wing section model data files used for SimFlow were STL files.

Pitch angles for a wing section (α_A) are the angle from horizontal (nose-up as positive) of the wing section's chord, where the chord is a straight line connecting the leading and trailing edges. In 2D simulations, the pitch angle of a point (α_P) on a curved line is the angle of the line tangent to the curve at the point of interest.

Air angle of attack (AoA) is the angle at which air's free stream velocity vector approaches the surface. Pressures near a surface can change air's velocity vector (i.e., bend the air's flow), and so, the AoA can change as it approaches a surface.

Turbulence was modeled using the RANS model using the k-ω SST modifications to simulate boundary layer separation, which the CFD model has been shown to be able to model effectively [31-33]. The results and discussion focus on pressure profiles rather than boundary layers, and the velocities tend to be lower than where boundary layers are dominant with low surface curvature [28].

CFD simulations using the RANS k-ω SST model are compared to laminar flow and Spalart-Allmaras models to identify the extent to which simulation of boundary layer separation impacts results.

A camber line is the line vertically halfway between the upper and lower surface from leading to trailing edge. The upper surface, lower surface, and camber line are considered to have the same camber for wing sections of this paper, and the terms "thin-plate cambered wing section" and "thin cambered wing section" are used synonymously. Camber and thickness of a wing section are typically specified as a fraction or percent of the chord length and may be abbreviated. A camber of 0.03 is also referred to as a 3% camber.

All images of pressure profiles use the symmetric color scale of Fig. 4 from blue through green to red with pressure in Pascals unless otherwise indicated.

Results

In the absence of ground-effect or enhancement from distributed propulsion, two trends characterize the performance of thin cambered wing sections:

- At low camber, a high L/D-efficiency has limited practical value due to low lift coefficients (i.e. low total lift forces).
- At higher camber, higher lift coefficients (i.e. high total lift forces) have limited value due to low L/D-efficiency.

The results are summarized by Figure 8 with further details in a supplement to this paper [17].

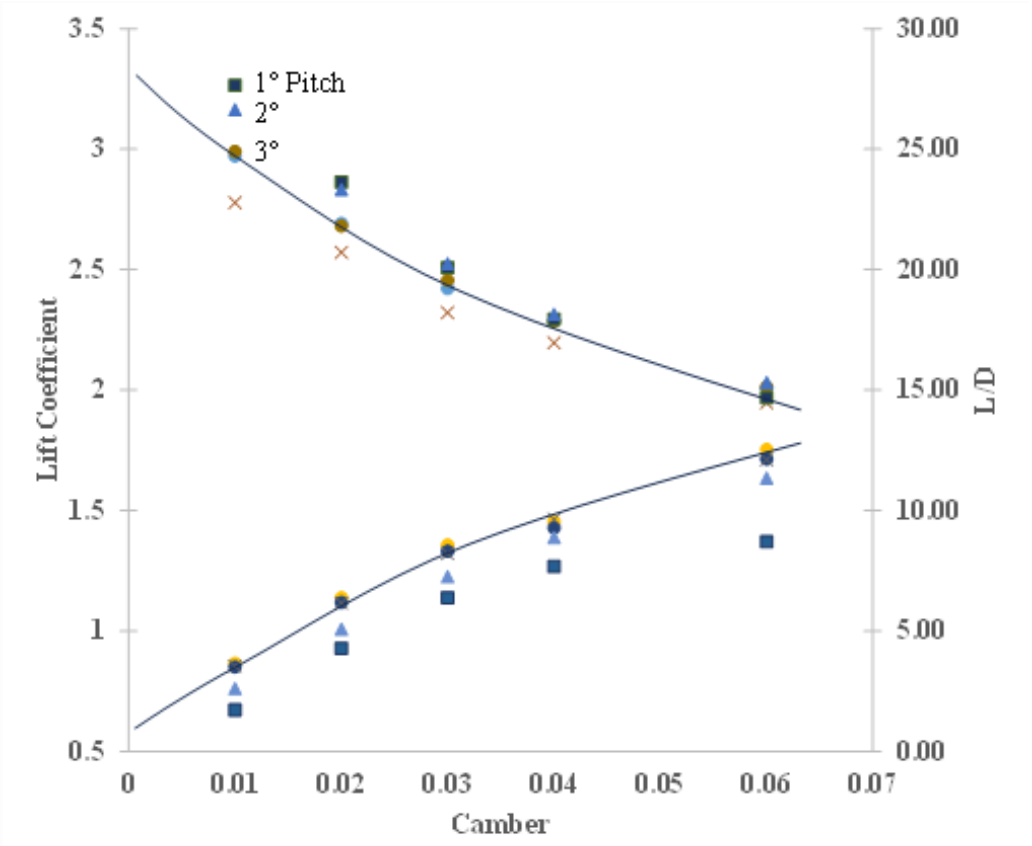

Figure 8. Impact of camber on lift coefficients and L/D on a thin cambered airfoil at constant camber.

For a higher-camber thin cambered airfoil, the thickness of the airfoil can be substantially less than the height. The likely explanation for the decrease in L/D with increasing camber for the 2D simulations is the increased form drag above the trailing airfoil section. The extent to which induced thrust of the forward section can compensate for induced drag of the aft section tends to decrease as height and/or thickness increase.

The 0.06 camber airfoil was selected for further study due to the higher lift coefficients at 0.06 camber versus lower cambers. While the L/D efficiency is less than with lower cambers, ground effect should increase this L/D by blocking the vertical loss of lift pressures, similar to the wing sections of Figures 4 and 5.

This anticipated trend is verified by the data of Figure 9, which identifies that L/D in excess of 70 are possible for wing sections. Robust leading and trailing stagnation points form with the increasingly robust formation of a higher-pressure region under the airfoil; the lift coefficients are consistently in excess of 1.0. Ground effect enhancements are able to substantially improve both lift and L/D-efficiency of thin cambered wing sections versus free flight.

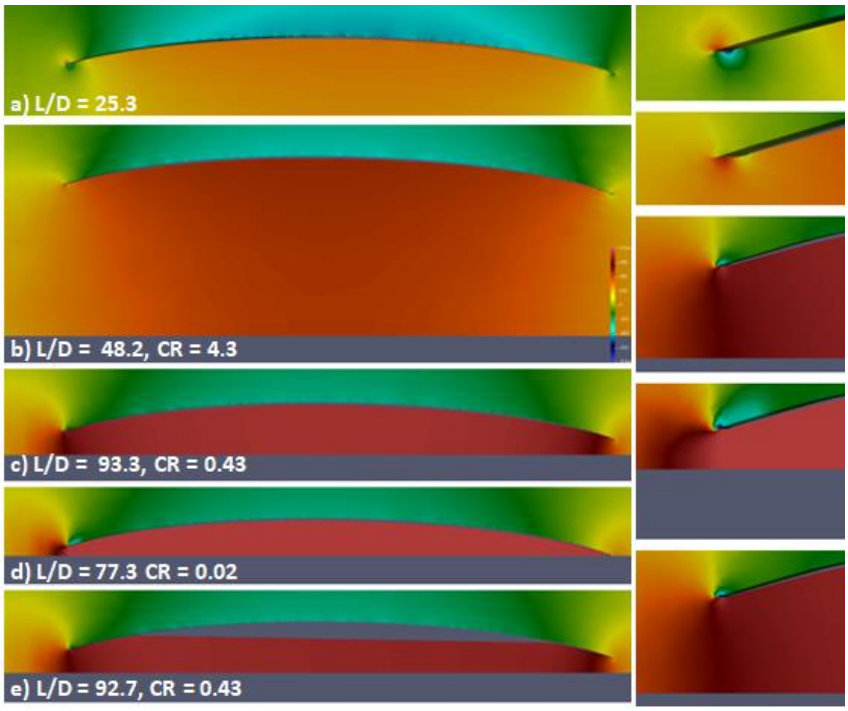

Figure 9. Pressure profiles of study on simple 0.06 camber airfoil at 1° pitch.

Each airfoil of Figure 9 has an expanded view of the leading edge. For the central profile (CR = 0.43), the lower surface of the leading edge has higher pressure and the upper surface has a lower pressure; hence both the upper and lower surfaces at the leading edge produce lift and thrust. The term “induced thrust” is used to refer to thrust resulting from pressures acting on wing section surfaces; the phenomenon occurs frequently as a mechanism enhancing high L/D efficiency and warrants a dedicated term.

For the Figure 9 wing sections, horizontal force on the leading section ranges from induced drag to induced thrust as the L/D efficiency varies from 25 to >90. Methods of increasing induced thrust on the front section include: a) distributed propulsion, including Lift Span Tech, b) increasing the pitch of the wing section, and c) optimizing the position of a leading-edge slat.

Advantages of a thin camber lifting body design include:

- Use of ultra-light weight panels or sheets for large sections of the lifting body.

- Use of bifacial solar panels for large sections of the lifting body.
- Compatibility with designs allowing for lateral and/or longitudinal expansion of the lifting body area.
- Synergy of the crossover propulsor illustrated by Figure 10.

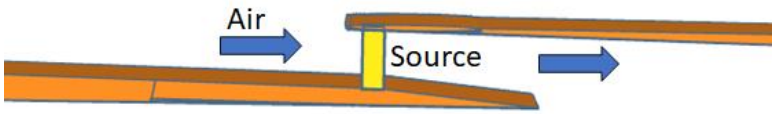

Figure 10. Illustration of crossover propulsor with intake above an upper airfoil and discharge below a trailing airfoil.

Cambered Panel Performance in Ground-Effect Flight – The cross-over source of Figure 10 is basically a spanwise ducted-fan sequence where the duct's upper surface continues as a thin trailing airfoil. The pressure profiles (Figure 11) illustrate how higher pressures can fill the chamber formed by the wing section. The 2D simulations effectively simulate a perfect fence, preventing all lateral losses of lift pressures. This efficiency can be approached in practice with a lower cavity and fences for low ground clearance.

The crossover propulsion source is defined to have horizontal flow which is substantially transformed to diffuse (i.e., non-directional) pressure in the chamber. The pressure in the chamber is a steady-state condition where air impacting the lower surface causes air's dynamic pressure to transform into static pressure; once the pressure forms at the surface, it dissipates. The transformation of translational/velocity energy to pressure energy includes air flows of different directions impacting, as well as air flows impacting surfaces as described by Principle 1.

Table 2 summarizes C_m, L/D, and representative chamber pressures. The crossover propulsor increases pressure in the chamber; however, at zero power setting for the crossover propulsor the gap in the wing section reduces L/D efficiency and the free stream velocity has a greater impact. In a consistent trend with other GEFT airfoils, the formations of robust leading-edge and trailing-edge stagnation points have significant impact on forming higher pressures within the chamber.

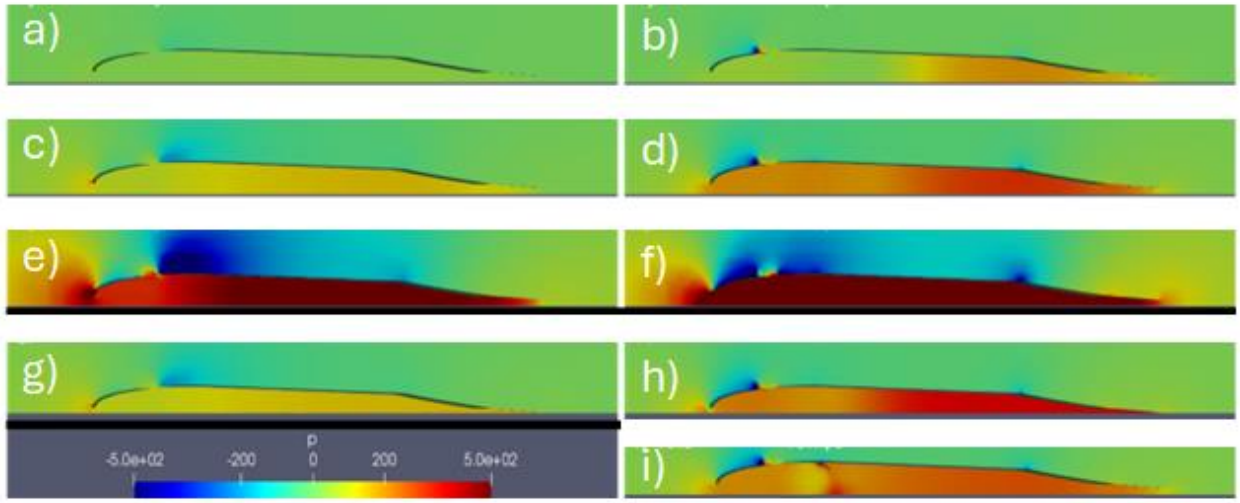

Figure 11. Illustration of pressure profile simulations of thin cambered wing sections at the centerline of Figure 1 digital prototype at the following settings. Clearance Ratio: a-f) 0.22; g-h) 0.02. Free stream velocity: a-b) 10m/s; c-d, g-h) 20m/s; e-f) 40m/s. Crossover propulsor settings: left column) No propulsor; Right column) 100 m^4/s^2 propulsor setting. i) Lower right image illustrates the baffle on the lower surface of a thin-cambered panel at 0.22 CR and 40m/s.

Table 2. Performance of Figure 11 thin cambered panel chamber (control, no crossover gap), with crossover propulsor to chamber (Crossover), and with both crossover propulsor and baffle. The control has no crossover gap in the wing section. C_m is cm from the front for a 1 m chord.

	Free Stream	Propulsor	CR	Cm	L/D	P
Control	40	0	0.22	18.1	88.6	684.0
Control	40	20	0.22	18.3	90.1	688.9
Control	40	100	0.22	18.7	87.9	702.1
Control	20	0	0.22	18.1	85.5	170.8
Control	20	20	0.22	18.6	84.5	174.7
Control	20	100	0.22	19.4	58.4	179.3
Control	10	0	0.22	18.1	82.4	42.7
Control	10	20	0.22	19.3	59.2	42.7
Control	10	100	0.22	19.6	22.0	44.6
With Baffle	40	0	0.22	16.2	24.7	572.1
With Baffle	40	20	0.22	16.7	33.0	606.0
With Baffle	40	100	0.22	19.3	80.6	735.4
With Baffle	20	0	0.22	16.2	24.4	142.6
With Baffle	20	20	0.22	18.7	72.5	177.1
With Baffle	20	100	0.22	26.2	40.9	231.6
With Baffle	10	0	0.22	16.1	24.0	35.5
With Baffle	10	20	0.22	24.2	46.6	54.7
With Baffle	10	100	0.22	57.4	14.1	123.3
Crossover	40	0	0.22	15.8	24.4	541.1
Crossover	40	20	0.22	16.4	32.8	583.9
Crossover	40	100	0.22	19.5	81.4	754.2
Crossover	20	0	0.22	15.7	24.1	134.8
Crossover	20	20	0.22	18.7	72.6	177.5
Crossover	20	100	0.22	28.1	43.9	207.4
Crossover	10	0	0.22	15.7	23.7	33.6
Crossover	10	20	0.22	25.9	49.0	53.1
Crossover	10	100	0.22	58.7	17.2	47.8

Figure 12 elucidates more subtle trends in performance. At zero propulsor power the crossover gap of the wing section decreases chamber pressure versus in the absence of the gap. For this airfoil, the gap should close to a smooth surface when air's dynamic pressure is enough to provide suspension.

L/D efficiency is higher for the control (see Figure 13). At higher propulsion powers, the baffle increased performance relative to the control and simple chambers by directing pressures more forward within the chamber. The baffle of this prototype was a simple flat plate; the evidence indicates that the shape of the chamber could be optimized with modified surfaces that direct flow to balance form drag in the chamber: directing pressure towards surfaces where higher pressures cause forward force.

As the propulsor power increases, L/D efficiency initially increases then decreases. Higher L/D performance of the cambered panel section correlates with the higher pressure expressed evenly throughout the lower surface [16]. The decreasing L/D efficiency with the crossover propulsor can be attributed to increased form drag due to higher pressures on the back half of the lower surface than the front half.

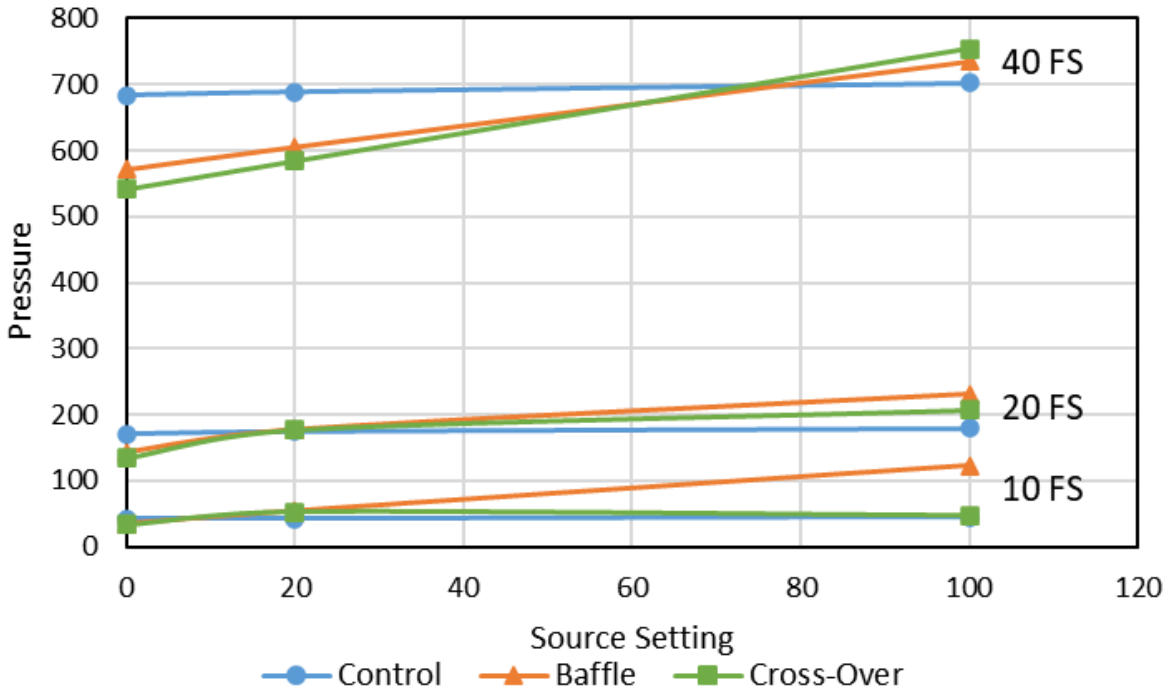

Figure 12. Impact of crossover propulsor ("Source", m^4/s^2) setting on average pressure (Pa) of cambered wing section. Trend lines are for data of Table 2.

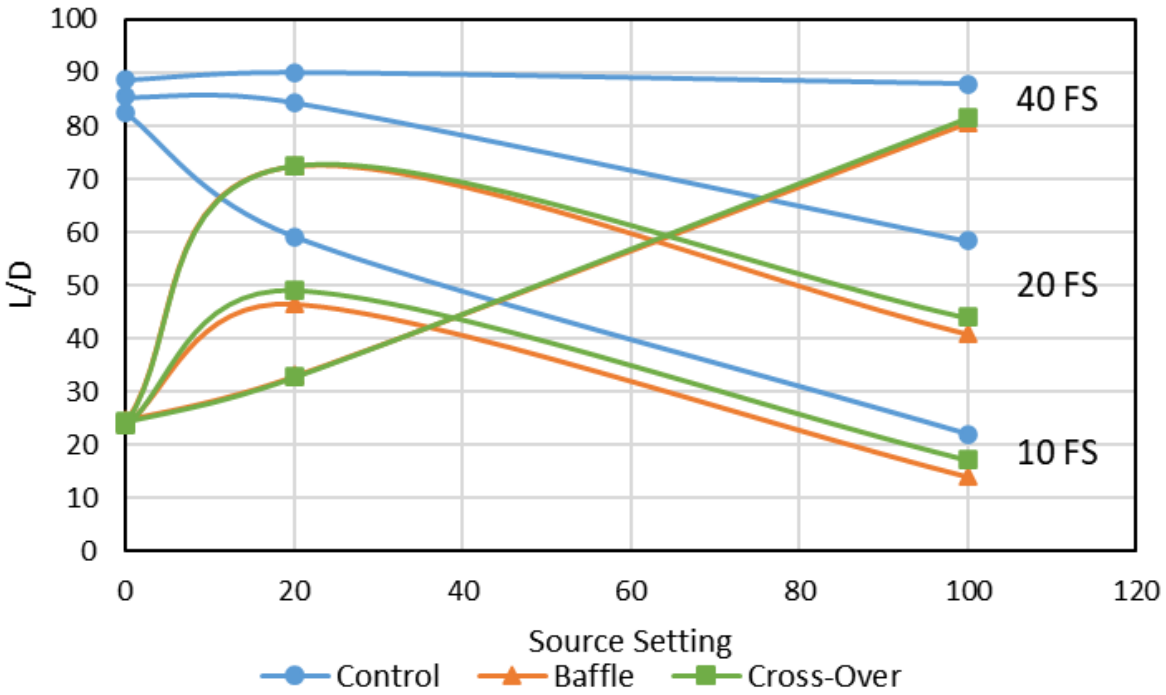

Figure 13. Impact of crossover propulsor ("Source", m^4/s^2) setting on L/D efficiency of cambered wing section. Trend lines are for data of Table 2.

Table 3. Performance of thin cambered panel chamber (control) without propulsor and crossover propulsor to chamber (Crossover), both at clearance ratio 0.02. Data provide comparison to Table 2 data which are at a higher ground clearance.

Wing section	Velocity	S (m^4/s^2)	Clearance ratio	Pressure	Cl	Cd	L/D
Control	40	0	0.02	818	1.231	0.0109	113.4
Crossover	40	0	0.02	537	0.867	0.0354	24.5
Crossover	40	20	0.02	585	0.922	0.0308	30.0
Crossover	40	100	0.02	818	1.227	0.0148	83.2
Control	20	0	0.02	205	1.236	0.0115	107.7
Crossover	20	0	0.02	134	0.868	0.0357	24.3
Crossover	20	20	0.02	199	1.201	0.0169	71.3
Crossover	20	100	0.02	308	1.765	0.0402	43.9
Control	10	0	0.02	51	1.241	0.0121	102.1
Crossover	10	0	0.02	33	0.869	0.0361	24.1
Crossover	10	20	0.02	71	1.636	0.0325	50.4
Crossover	10	100	0.02	228	4.711	0.1931	24.4

Because thin-cambered panels are more-reliant on pressures reaching the forward sections of the lower surface to cause induced thrust, the performance of a chamber is more dependent on blocking spanwise losses of higher pressures from the chamber. Table 3 presents wing section data at lower ground clearances which lead to higher chamber pressures from higher crossover propulsor settings.

A slat near the same ground clearance as the trailing edge gap would be effective in increasing L/D by increasing clearance to diminish induced drag on that slat—which would be the leading section of the chamber. The optimal shape and setting of that slat can be attained with results-driven optimization of the flap shape and setting.

Advantages of the chamber with a thin upper panel include: a) light weight and b) more straight-forward designs to allow spanwise extendable inboard sections to increase lift. Data identify that the highest L/D efficiencies are attained when the induced thrust on the cavities forward section is equal to the induced drag on the trailing section; a horizontal lower surface forward the trailing flap achieves the same objective. Previous work identifies the approach to designing GEFT with horizontal upper surfaces of cavities [15].

Figure 14 summarizes performance of the 3D prototype with a cavity having a horizontal upper surface extending from the leading edge to the trailing flap. A low L/D, 5.2, in free flight can be attributed to a lack of optimization of the upper wing with lateral

extensions. The base case design of Figures 1 and 14 has wings of minimal lateral extension suitable for flight in railway corridors with width restrictions [29]. A Clearance Ratio of 0.02 is reasonable above surfaces like railway tracks, translating to a 2.5 cm clearance gap for a cabin wing section 2.5 m high.

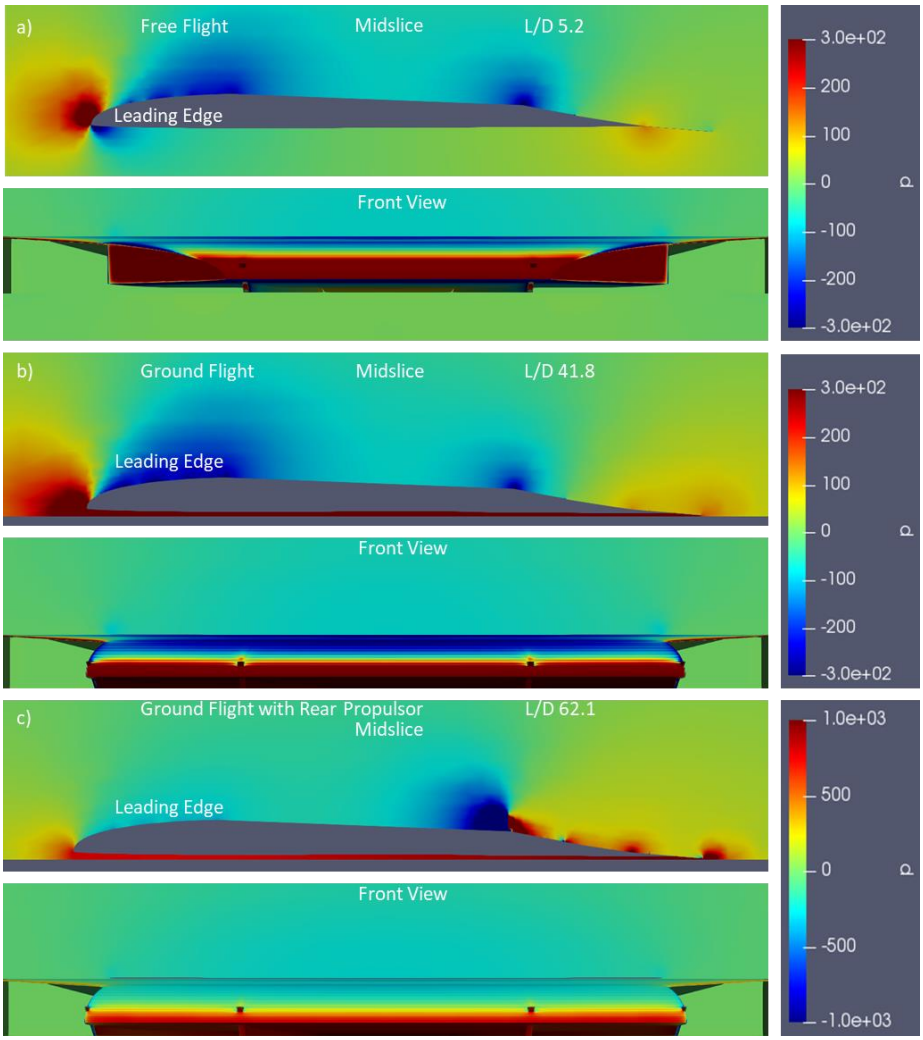

Figure 14. Simulated flight of the 6.4m long 3D model from Figure 1 at three conditions: a) free flight without propulsor, b) 0.02 clearance ratio flight without propulsor, and c) 0.02 clearance ratio flight with strong (2000 m^4/s^2) trailing propulsor.

Impact of Catamaran Design – Subsequent Figure 15 and Table 4 summarize performances of the Figure 1 prototype with the following modifications: a) no upper lateral wing extensions, b) an aspect ratio of 0.5 with chord length of 1 m, c) a thin-cambered inboard section at 0%, 40%, 60%, and 100% of the span, d) clearance ratios of 0.02 and 0.1, e) a 40 m/s free stream velocity, and f) Lift Span propulsor settings as indicated.

Within digital experiment accuracy the, 0%, 40%, and 60% inboard chamber span digital prototypes exhibited the same performance. Figure 16 shows how the surface pressure profiles of the three configurations are substantially the same.

For the thin-cambered airframe with fences, i.e. 100% chamber inboard, the 0.1 clearance ratio had a consistently lower L/D indicating that there was greater lateral loss of lift forces from the chamber. This can be attributed to the filled camber having a lower open area below the lower surface for flux losses of lift pressure.

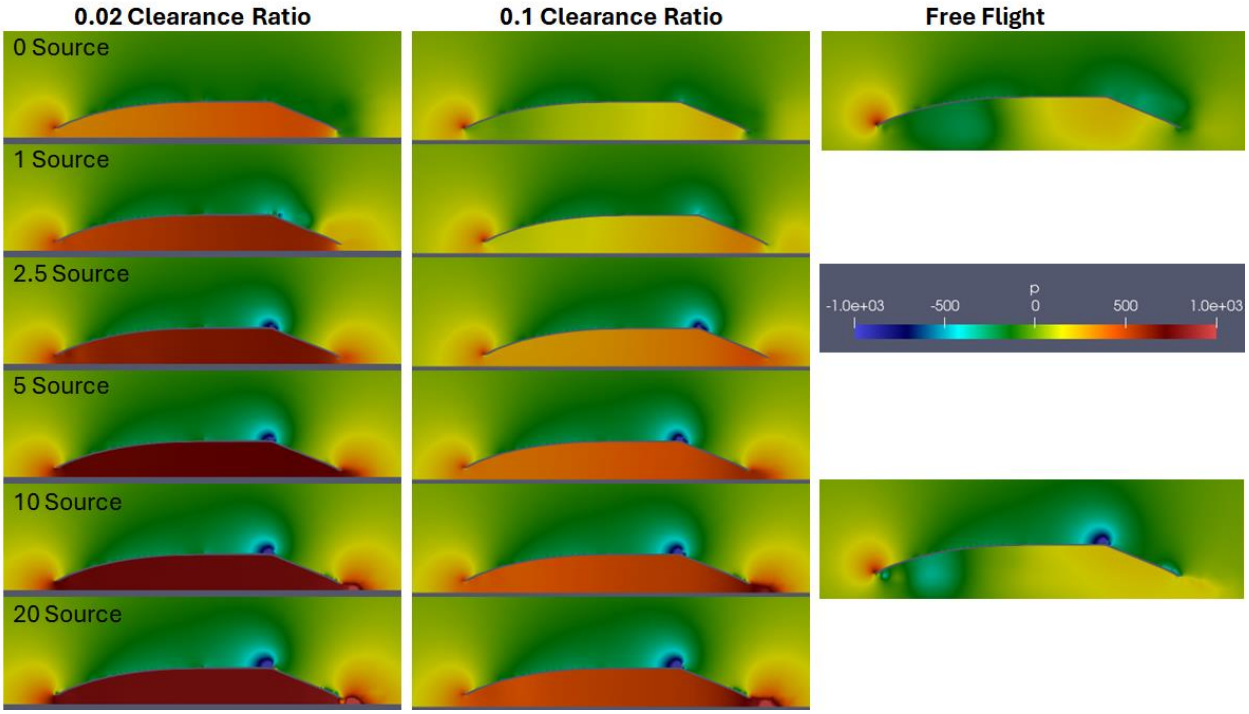

Figure 15. Pressure profiles of GEFT digital prototype with 60% panel thin-cambered midsection at conditions of Table 4.

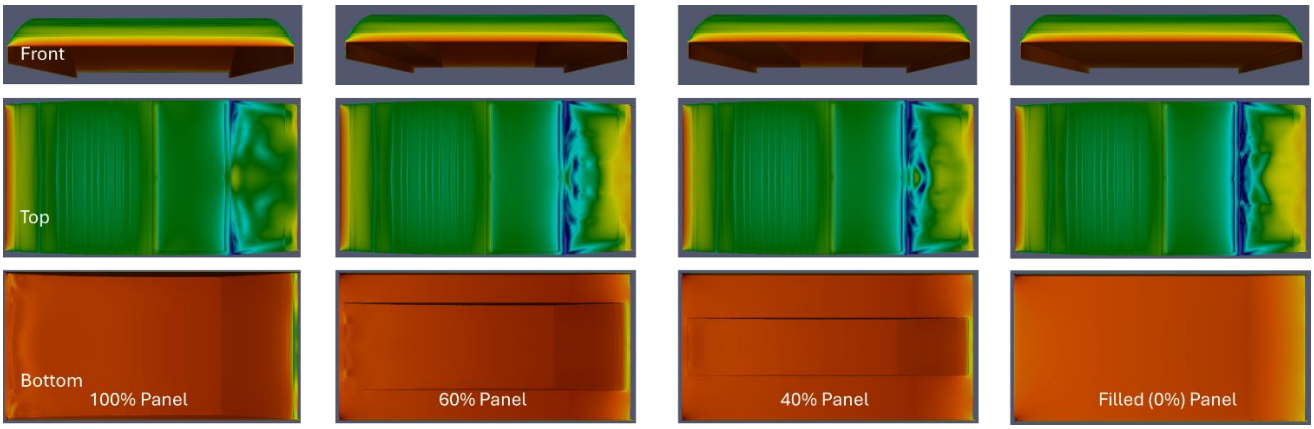

Figure 16. Pressure profiles of surfaces of 0%, 40%, 60%, and 100% inboard chamber span digital prototypes. Data is at 1.0 m^4/s^2 Source and 0.02 clearance.

Table 4. Summary of L/D and cavity pressure values for GEFT with thin-cambered inboard section at free stream velocity of 40 m/s, 0.5 aspect ratio, and horizontal upper surface of cavity.

Inboard Chamber Span	CR	Source	Cl	L/D
60%	>1000	0	0.22	2.4
60%	>1000	10	0.41	3.5
60%	0.02	0	0.75	15.8
60%	0.02	1	1.06	26.4
60%	0.02	2.5	1.20	38.2
60%	0.02	5	1.39	43.4
60%	0.02	10	1.52	41.6
60%	0.02	20	1.62	34.6
60%	0.1	0	0.33	5.9
60%	0.1	1	0.52	9.3
60%	0.1	2.5	0.75	15.6
60%	0.1	5	0.92	17.6
60%	0.1	10	1.05	17.2
60%	0.1	20	1.15	15.9
40%	0.02	0	0.70	14.9
40%	0.02	1	1.02	27.2
40%	0.02	2.5	1.18	38.2
40%	0.1	0	0.28	5.5
40%	0.1	1	0.41	7.8
40%	0.1	2.5	0.72	16.6
0%	0.02	0	0.62	14.6
0%	0.02	1	0.92	29.6
0%	0.02	2.5	0.00	40.2
0%	0.1	0	0.26	5.7
0%	0.1	1	0.39	8.2
0%	0.1	2.5	0.65	17.1
100%	0.02	0	0.82	16.2
100%	0.02	1	1.02	21.6
100%	0.02	2.5	1.24	38.3
100%	0.1	0	0.38	5.4
100%	0.1	1	0.50	7.6
100%	0.1	2.5	0.76	14.2

Table 5. Summary of L/D and cavity pressure values for GEFT with thin-cambered inboard section at free stream velocity of 40 m/s, 1.0 aspect ratio, and horizontal upper surface of cavity.

Inboard Chamber Span	CR	Source	Cl	L/D
60%	0.02	0	1.73	18.6
60%	0.02	1	1.87	21.7
60%	0.02	2.5	2.49	42.5
60%	0.1	0	1.13	10.4
60%	0.1	1	1.22	11.7
60%	0.1	2.5	1.51	15.0

As identified by Table 5, increasing the aspect ratio from 0.5 to 1.0 leads to a higher L/D. Aspect ratio can be increased to increase L/D efficiency, approaching the efficiency of wing sections by reducing lateral pressure losses, however, the lower aspect ratios with filled camber are likely to be more robust against tidal forces for extended sea deployment with improved access to harbors and channels.

Discussion

Rapid advances in ground effect machine design have been enabled by a science of aerodynamic lift that includes six basic physics principles useful for interpreting and extrapolating CFD simulation results. As a consequence of these advances, a discussion of results relies on multiple paper pre-prints on the topics of: a) science of aerodynamic lift with causality [3], b) ground effect flight technology (GEFT) approaches to design [14], and c) critical data and thinking in ground effect vehicle design [30]. This paper extends upon the foundation of these other papers on the topic of using thin cambered inboard sections in GEM aircraft.

Thin Cambered Inboard Sections - For simple thin cambered wing sections, the highest L/D efficiencies are only achieved when higher pressures under the camber extend from leading to trailing edge at pitch angles near 1°. In ground-effect flight the ground blocks downward dissipation of lift forces and makes these higher efficiencies attainable. For lifting body fuselages consistent with passenger cabins and heavier payloads, induced drag on the upper surface can be overcome with Lift Span Tech.

Several design parameters impact L/D efficiency of cambered-panel sections, including: a) baffle surfaces to reduce changes in pressure from leading to trailing lower surfaces, b) extendable slats to change the effective pitch of cambered section, c) leading edge shapes of the cambered panel sections, and d) crossover fan locations, intake/discharge surfaces, and transition ability to streamline flows when air's dynamic pressure is sufficient to sustain full aerodynamic lift. The effectiveness of a crossover propulsor was limited by higher ground clearances where the optimal clearances of fences and flaps for WIG operation (i.e., using oncoming air's dynamic pressure to create

lift) are greater than clearances for hovercraft type of operation.

Of these “a-d” degrees of freedom, the ground effect and Lift Span Tech with adjustable fences in ground effect had the most profound impact on L/D efficiency when using previously-identified GEFT design approaches [14, 15, 31]. This work does not suggest the impact of these “a-d” degrees of freedom and lateral wings are unimportant, but rather, more results-driven optimization topics applicable to different operating parameters than this work. In particular, these other degrees of freedom are important for higher or lower ground clearance operation.

The significance of thin cambered mid-sections of a GEFT aircraft is the ability to increase lift with minimal increase in vehicle weight; the thin cambered midsection panel functions as an ultralight high L/D inboard wing section.

Also, the panels could be solar panels. The addition of solar panels which provide lift in an ultralight format sets the stage to scale to larger vehicles where increasing amounts of energy is provided by solar panels.

As the scale of the vessel increases, the camber may increase which increases L/D efficiency at a constant ground clearance. Also, as the scale increases, the inadvertent impact of side fences with water has reduced relative impact on the aircraft due the ratio of fence perimeter to lift surface area decreasing with increasing scale. Pushing the limits of low air gaps increases L/D. These trends indicate that exceptionally efficient GEM aircraft are possible at larger sizes, and that the benefits of increased efficiency can be compounded by increased surface area for collection solar power.

Free Flight - Thin cambered airfoils at low aspect ratios perform poorly in free flight with typical solutions being to: a) optimize vehicle pitch and b) add laterally-extending wings. The downward and spanwise dissipation of lift for low aspect ratio designs is significant in free flight. Three approaches to free flight make applicable sense for GEFT technology: 1) designs where free flight is less than 5% of the transit with ground effect dominating translation with targeted free flight L/D of similar to helicopters at about 6.0, 2) use of retractable wings and Lift Span Tech to increase free flight efficiency to L/D efficiencies in excess of 15, and 3) use of expandable chamber technology and Lift Span Tech to increase L/D efficiencies in free flight. These are topics of results-driven optimization that are highly dependent on application.

Conclusions

A GEFT ground effect machine uses a trailing section propulsor configured with a trailing taper, referred to as Lift Span Tech, to overcome induced drag issues that have limited the effectiveness of GEM. In ground effect, GEFT are able to achieve L/D efficiencies twice that of past GEM. Thin cambered wing sections of the GEFT design are able to achieve similar L/D efficiencies in ground effect in low aspect designs that have poor performance in free flight. Efficiency correlated with [clearance]:[height], where in the preferred design the clearance is a constant clearance of cavity fences with the ground and the height is the fuselage height of a lifting body GEM.

A catamaran design was evaluated where an inboard thin-cambered section was placed between two outboard wing section where the cambered was filled to a flat lower surface. Within the accuracy of the digital prototypes, the thin cambered inboard section did not reduce L/D efficiency. Design advantages of a thin cambered inboard section include increased lift per kg of wing section and the ability to reasonably make the inboard

span expandable and retractable. For spanwise expandable GEM retracted configurations would provide improved corridor access and increased robustness against tidal forces while an expanded configuration would provide higher L/D efficiency in flight through wider corridors. When conditions warrant, an expandable inboard section can be configured with solar panels where extension increases solar energy collection.

The effectiveness of a crossover propulsor was limited by higher ground clearances where the optimal clearances of fences and flaps for WIG operation (i.e., using oncoming air's dynamic pressure to create lift) are greater than clearances for hovercraft type of operation. Whereas sea planes are typically not suitable for extended deployment at sea, GEM with expandable inboard sections could be designed to be as stable as other boats and ships for extended deployment at sea.

Appendix Summary of Supplementary Materials

The following are supplemental materials with preliminary findings and trends which created the foundation for this work and elucidate details beyond what is available in this text:

Supplement #1 - Suppes A.B., Suppes G.J. Understanding Thin Cambered Wing sections and their Solar Aircraft Applications, Nov-2023.

Supplement #2 - Suppes A.B., Suppes G.J. Thermodynamic Analysis of Distributed Propulsion, Submitted to Energy, Nov-2023.

References

[1] Halloran, M., and O'Meara, S., "Wing in Ground Effect Craft Review," Aeronautical and Maritime Research Laboratory, Melbourne Victoria 3001 Australia, 1999. https://apps.dtic.mil/sti/pdfs/ADA361836.pdf

[2] Davis, S.C., Boundy, R.G., "Transportation Energy Data Book," Oak Ridge National Laboratory, 2022,

[3] Suppes, A., Suppes, G., Lubguban, A., and Al-Maomeri, H., "An Airfoil Science Including Causality," *Cambridge Engage,* 2024, 10.33774/coe-2024-w4qtp

[4] Bulat, P., Chernyshov, P., Prodan, N., and Volkov, K., "Control of Aerodynamic Characteristics of Thick Airfoils at Low Reynolds Numbers Using Methods of Boundary Layer Control," *Fluids,* Vol. 9, No. 1, 2024, pp. 26. 10.3390/fluids9010026

[5] Anonymous "Pilot's Encyclopedia of Knowledge," Skyhorse Publishing, Inc, 2007, pp. 3–8.

[6] Hurt, H.H.J., "Aerodynamics for Naval Aviators," USAF, 1965,

[7] Correspondents, B.N.N., "Liberty Lifter: DARPA's Ground Effect Aircraft Revolution," 2023https://bnnbreaking.com/tech/liberty-lifter-darpas-ground-effect-aircraft-revolution [cited Feb 12 2024].

[8] Suppes, G., and Suppes, A., "Ground Effect Vehicle," Vol. PCT/US24/35242, 2024, pp. 1–32. www.hs-drone.com

[9] Blain, L., "Regent to debut its hydrofoiling ground-effect Seagliders in Hawai'i," Jan 212024https://newatlas.com/aircraft/hawaii-seaglider/ [cited Mar 8 2024].

[10] Anonymous "AIRFISH 8," 2023https://www.wigetworks.com/airfish-8 [cited Mar 4 2024].

[11] Suppes, G.J., "Flat plate airfoil platform vehicle," Vol. PCT/US2021/016392, No. WO 2021/226551 A2, 2021, pp. 1–25. http://www.terretrans.com/uploads/1/1/7/3/117309869/4_wo2021225651a2.pdf

[12] Suppes, G., "Glider Guideway System," Vol. US15808966, https://patents.google.com/patent/US20180057018A1/en

[13] Suppes, A., Suppes, G., Lubguban, A.A., and Al-Moameri, H.H., "Kinetic theory of gases: explanation of aerodynamic lift," *Aviation (in Review),* 2024,

[14] Suppes, G., and Suppes, A., "Ground Effect Flight Transit (GEFT) – Approaches to Design," Cambridge University Press, Cambridge Open Engage, 2024. https://www.cambridge.org/engage/coe/article-details/66b2340b01103d79c5e7ab2310.33774/coe-2024-2c87q

[15] Suppes, A., and Suppes, G., "Ground Effect Flight Transit (GEFT) – Towards Trans-Modal Sustainability," Vol. 1, 2024, https://doi.org/10.33774/coe-2024-prxvr

[16] Suppes, A., and Suppes, G., "Thermodynamic Analysis of Distributed Propulsion," *Research Square,* 2023, pp. 1–26. 10.21203/rs.3.rs-4670270/v1

[17] Suppes, G., and Suppes, A., "Understanding Thin Cambered Airfoils and their Solar Aircraft Applications," *Research Square,* 2023, pp. 1–29. https://doi.org/10.21203/rs.3.rs-4670250/v1

[18] Deline, C., Palaez, S.A., Marion, B., Sekulic, B., Woodhouse, M., and stein, J., "Bifacial PV System Performance: Separating Fact from Fiction," 2019https://www.nrel.gov/docs/fy19osti/74090.pdf [cited Nov 27 2023].

[19] Guerrero-Lemus, R., Vega, R., Kim, T., Kimm, A., and Shephard, L.E., "Bifacial solar photovoltaics – A technology review," *Renewable and Sustainable Energy Reviews,* Vol. 60, 2016, pp. 1533–1549. https://doi.org/10.1016/j.rser.2016.03.041

[20] Osei, Emmanuel Yeboah, Opoku, Richard, Sunnu, Albert K. Adaramola, Muyiwa S., "Development of High Performance Airfoils for Application in Small Wind Turbine Power Generation," *Journal of Energy,* Vol. 2020, 2020, https://doi.org/10.1155/2020/9710189

[21] Kim, H.D., Perry, A.T., and Ansell, P.J., "A Review of Distributed Electric Propulsion Concepts for Air Vehicle Technology," *2018 AIAA/IEEE Electric Aircraft Technologies Symposium (EATS),* 2018, pp. 1–21. 10.2514/6.2018-4998

[22] Gohardani, A., Doulgeris, G., and Singh, R., "Challenges of future aircraft propulsion: A review of distributed propulsion technology and its potential application for the all electric commercial aircraft," *Progress in Aerospace Sciences,* Vol. 47, 2011, pp. 369–391. 10.1016/j.paerosci.2010.09.001

[23] Finger, D., Braun, C., and Bil, C., "A review of configuration design for distributed propulsion transitioning VTOL aircraft," *2017 Asia-Pacific International Symposium on Aerospace Technology, Seoul, Korea,* 2017, pp. 1–15.

[24] Cole, J., Krebs, T., Barcelos, D., and Bramesfeld, G., "Influence of Propeller Location, Diameter, and Rotation Direction on Aerodynamic Efficiency," *Journal of Aircraft,* Vol. 58, 2020, pp. 1–9. 10.2514/1.C035917

[25] Ma, Y., Zhang, W., and Elham, A., "Multidisciplinary Design Optimization of Twin-Fuselage Aircraft with Boundary-Layer-Ingesting Distributed Propulsion," *Journal of Aircraft,* Vol. 59, 2022, 10.2514/1.C036559

[26] Serrano, J., Tiseira, A., García-Cuevas, L., and Varela, P., "Computational Study of the Propeller Position Effects in Wing-Mounted, Distributed Electric Propulsion with Boundary Layer Ingestion in a 25 kg Remotely Piloted Aircraft," *Drones,* Vol. 5, 2021, pp. 56. 10.3390/drones5030056

[27] Wu, R., Soutis, C., Zhong, S., and Filippone, A., "A morphing aerofoil with highly controllable aerodynamic performance," *The Aeronautical Journal,* Vol. 121, 2016, pp. 1–19. 10.1017/aer.2016.113

[28] Lee, D., Nonomura, T., Oyama, A., and Fujii, K., "Comparison of Numerical Methods Evaluating Airfoil Aerodynamic Characteristics at Low Reynolds Number," *Journal of Aircraft,* Vol. 52, 2015, pp. 296–306. 10.2514/1.C032721

[29] Suppes, A., and Suppes, G., "New Benchmarks in Ground-Effect Flight Energy Efficiency," July 102024https://www.researchsquare.com/article/rs-4707178/v1https://doi.org/10.21203/rs.3.rs-4707178/v1 [cited Jul 29 2024].

[30] Suppes, G., and Suppes, A., "Critical Data and Thinking in Ground Effect Vehicle Design," Cambridge University Press, Cambridge Open Engage, 2024. https://www.cambridge.org/engage/https://doi.org/10.33774/coe-2024-76mzx

[31] Suppes, G., and Suppes, A., "Ground Effect Flight Transit (GEFT) in Subways," Vol. 1, 2024, https://doi.org/10.33774/coe-2024-6w0lw